Hindawi
Shock and Vibration
Volume 2021, Article ID 6662686, 11 pages
https://doi.org/10.1155/2021/6662686

Research Article

Detection of Bolt Looseness Based on Average Autocorrelation Function

Jigang Wu,[1] **Jun Shao**,[1] **Gen Zhou**,[2] **Deqiang Yang**,[1] **and Yuan Cheng**[1]

[1]*Hunan Provincial Key Laboratory of Health Maintenance for Mechanical Equipment, Hunan University of Science and Technology, Xiangtan 411201, China*
[2]*AECC Hunan South Astronautics Industry Co, Ltd., Zhuzhou 412002, China*

Correspondence should be addressed to Jigang Wu; jwu@cvm.ac.cn

Received 23 November 2020; Revised 6 April 2021; Accepted 3 May 2021; Published 15 May 2021

Academic Editor: Francesco Pellicano

Bolted connections are widely used in multiple engineering fields including aerospace and mechanical engineering due to their numerous advantages like the ability to bear relatively heavy loads, low costs, easy installation, and implementation. Bolt looseness may lead to costly disasters in industries and some cases of injuries. A new method for bolt looseness detection based on average autocorrelation function is proposed. It does not usually directly extract the looseness damage feature from the original response signal to detect the bolt looseness, but it uses the average autocorrelation function value at time lag $T = 0$ of the vibration pixel displacement signal to establish the looseness damage index. In terms of structural arrangement of this paper, firstly, the theoretical background of the proposed method is given. Then, an experimental system for bolt looseness detection based on computer vision is designed, and a verification experiment is carried out with the bolted connection plate as the experimental object. The results show that the proposed method can effectively obtain the location of the looseness damage of the bolted connection plate, which provides a new technical reference for the online monitoring of the looseness damage of bolted connection plate.

1. Introduction

Bolted connections are widely used in multiple engineering fields including aerospace and mechanical engineering, because they have numerous advantages such as the ability to bear relatively heavy loads, low cost, and easy installation and implementation [1]. However, bolt looseness, induced by fatigue, impact, and thermal loads, may lead to costly disasters in industries and some cases of injuries [2, 3]. Therefore, for maintaining the healthy and stable operation of equipment, how to detect the bolt looseness simply and effectively as early as possible has attracted more and more attention by many researchers [4].

Nowadays, the methods of bolt looseness detection proposed by many researchers mainly include impedance-method methods [5–7], vibration-based methods [8–10], and ultrasonic-based methods [11–13]. In the impedance-based methods, the piezoelectric transducers (PZT) are usually attached to the surface of a target structure being inspected [14]. Representatively, Lee [15] attempted a novel technique to detect bolt looseness using a transfer impedance technique for monitoring the structural health of a bolt joint. In addition, Sun and Zhang [16] proposed a monitoring method based on an impedance method that was researched for bolt looseness of steel structure. However, the impedance-based measurement method has high cost of the installation sensors. Moreover, in the vibration-based methods, representatively, Razi et al. [17] introduced a vibration-based health monitoring strategy for detecting the loosening of bolts in a pipeline's bolted flange joint. They conducted numerical and experimental studies to verify the feasibility of the proposed method. Huda et al. [18] investigated a vibration testing and health monitoring system based on an impulse response excited by laser ablation. Furthermore, they also estimated the bolt loosening by detecting fluctuations of the high frequency response with

their health monitoring system. In addition, Esmaeel et al. [19] explored a novel vibration-based damage detection methodology using the empirical mode decomposition (EMD) to calculate the energy damage index (EDI) in common industrial bolted joints. Additionally, in the ultrasonic-based methods, representatively, Zhang et al. [20] presented a bolt looseness recognition method based on the subharmonic resonance analysis. Furthermore, they also carried out analytical prediction and numerical simulations to verify the validity of the loosening detection method for bolted joint structures. Amerini and Meo [21] developed a tightening/loosening state index based on the first-order acoustic moment for the linear acoustic/ultrasound method. In addition, Fierro and Meo [22] proposed an in situ structural health monitoring approach based on the evaluation of linear and nonlinear modulated acoustic moments for the assessment of the loosened state of bolts. However, the ultrasonic-based method lacks accuracy due to the use of linear phenomena such as reflection and scattering [23].

The vibration-based method is simple in principle and easy to operate, and its measurement principles are mainly divided into two aspects: the first aspect is that the stiffness of the bolted connection is reduced by bolt looseness, which will result in the changes of the dynamic characteristic parameters (natural frequencies, damping ratio, and mode shapes) of the structure, and the second aspect is that the various signal processing methods are used to process the signals obtained from the sensors attached to the structure to extract the damage feature information of the structure. He and She [24] developed a new identification method for bolt looseness in wind turbine towers for preventing the collapse of wind turbine towers. They found that the natural frequencies, damping ratio, and vibration characteristics are not very sensitive to the looseness of flange bolts, so they used the first-order phase difference curve to find the bolt looseness of the flanges. Vibration tests and analyses were carried out on six wind turbine towers with loose bolts, which verified their feasibility of the proposed method. Zhou et al. [25] formulated an energy-based damage index based on the high-frequency intrinsic mode functions. They conducted a vibration test on the frame structure, and experimental results showed that the energy-based damage index can accurately detect bolt looseness damage. Chen et al. [26] proposed a looseness diagnosis method for connecting bolt of fan foundation based on sensitive mixed-domain features of excitation response and manifold learning. They verified the feasibility of the proposed method with experimental results. Pnevmatikos et al. [27] selected the difference of the wavelet coefficients of the acceleration response of the healthy and loosened connection structure as an indicator of the damage and presented an application of wavelet analysis for damage detection of steel frames with bolted connections. The feasibility of the wavelet approach to damage detection was verified through experiments. He and Zhu [28] proposed using structural natural frequency changes to detect the loosening of bolted connections. They took the steel pipe structure with bolted flanges as the experimental object and successfully detected the position of the loose bolts. Milanese et al. [29] explored two signal processing techniques to use in assessing the connection strength. The first method relied on basic statistical properties of the measured strains and their time derivatives, and the second method was based on power of the signal in different frequency bands. They also verified the feasibility of the proposed methods by experimental studies.

In general, the vibration-based methods mentioned above in [28, 29] can be used to identify bolt looseness. It is mainly based on the dynamic characteristic parameters or the signal processing methods to establish the damage index (DI). However, when the degree of bolt looseness damage is small, the change of the structural dynamic characteristic parameters is not very obvious. Further, the signal processing methods proposed in [9, 25, 26] can be usually implemented to detect the bolt looseness only when the input is confirmed. Actually, when the device is in operation, it means that the detailed information of the input is unknown, so how to recognize looseness based on ambient excitation is an important key affair. Since the excitation of the structure is unknown under operating conditions, taking into account the relevant theory of Natural Excitation Technique (NExT) in [30, 31], the vibration response characteristics of the structure are analyzed under ambient excitation. Moreover, it is found that the autocorrelation function of the structural vibration displacement response is related to the structural modal parameters. Based on this reason, this paper proposes using the autocorrelation function of vibration response to establish damage index (DI) for detecting the bolt looseness.

The remaining sections of this paper are as follows. The theoretical background of the response analysis under natural excitation, the definition of looseness damage index, and the proposed method with procedures are introduced in Section 2. The design principle of the experimental system and the experimental method are described in Section 3. The results are discussed in Section 4 to demonstrate the feasibility of the proposed method. At last, some conclusions are drawn in Section 5.

2. Theoretical Background

2.1. Response Analysis under Natural Excitation. For a structural dynamics system with n degrees of freedom (DOFs), the dynamic equation describing the characteristics of the system can be expressed as [30, 31]

$$\mathbf{M}\ddot{x}(t) + \mathbf{C}\dot{x}(t) + \mathbf{K}x(t) = \mathbf{f}(t), \tag{1}$$

where $\boldsymbol{M}$, $\boldsymbol{C}$ and $\boldsymbol{K}$ are the mass matrix, damping matrix, and stiffness matrix of the structure with the dimension of $n \times n$, respectively. $\boldsymbol{x}(t)$ is the displacement vector of the structure response, and $\boldsymbol{f}(t)$ is the excitation vector of the structure.

Because the response of the linear time-invariant system can be expressed as the product of the mode shapes and the modal coordinates, the structural response can be written as

$$x(t) = \mathbf{\Phi}\mathbf{q}(t) = \sum_{r=1}^{n} \varphi_r q_r(t), \tag{2}$$

where Φ is the modal matrix composed of the modal vectors, $\boldsymbol{q}(t)$ is the vector of modal coordinates, $q_r(t)$ is the r^{th} modal coordinate value, φ_r is the r^{th} mode shape, and n is the number of DOFs.

Since real normal modes are assumed, $\boldsymbol{M}$, $\boldsymbol{C}$, and $\boldsymbol{K}$ are diagonalized. Next, substituting equation (2) into equation (1) will result in the following [30].

$$\left(\ddot{q}_r(t) + 2\zeta_r\omega_{nr}\dot{q}_r(t) + \omega_{nr}^2 q_r(t)\right) = \frac{1}{m_r}\varphi_r^T f(t), \tag{3}$$

where ω_{nr} is the r^{th} modal frequency, ζ_r is the r^{th} modal damping ratio, m_r is the r^{th} modal mass, and $r = 1,\ldots, n$.

Assume that, under the zero initial condition, we use Duhamel's integral to solve equation (3), and it will be obtained that

$$q_r(t) = \int_{-\infty}^{t} \varphi_r^T f(\tau) g_r(t-\tau)\mathrm{d}\tau, \tag{4}$$

Substituting equation (4) into equation (2) results in the following.

$$x(t) = \sum_{r=1}^{\mathrm{n}} \varphi_r \int_{-\infty}^{t} \varphi_r^T f(\tau) g_r(t-\tau)\mathrm{d}\tau, \tag{5}$$

From equation (5), it can be obtained that if the excitation is $f_k(t)$ at point k on the system, the vibration response $x_{ik}(t)$ at point i can be expressed as

$$x_{ik}(t) = \sum_{r=1}^{n} \varphi_{ir}\varphi_{kr} \int_{-\infty}^{t} f_k(\tau) g_r(t-\tau)\mathrm{d}\tau, \tag{6}$$

where $x_{ik}(t)$ is the vibration displacement response at point i, $f_k(t)$ is the excitation at point k, φ_{ir} is the r^{th} mode shape value at point i, φ_{kr} is the r^{th} mode shape value at point k, and n is the number of DOFs. $g_r(t)$ is the impulse response function related to the r^{th} modal parameters of the system. In addition, $g_r(t)$ is

$$g_r(t) = \begin{cases} \dfrac{1}{m_r\omega_{dr}} e^{-\zeta_r\omega_{nr}t}\sin\left(\omega_{dr}t\right), & t \geq 0, \\ 0, & t < 0, \end{cases} \tag{7}$$

where m_r, ζ_r, and ω_{nr} are the r^{th} modal mass, modal damping, and modal frequency, respectively. ω_{dr} is the r^{th} damped modal frequency, $\omega_{dr} = \omega_{nr}\sqrt{(1-\zeta_r{}^2)}$.

Based on the definition of autocorrelation function, the autocorrelation function $R_{iik}(T)$ of the vibration displacement response at point i with the time lag T is

$$R_{iik}(T) = E\left[x_{ik}(t+T)x_{ik}(t)\right], \tag{8}$$

where $E[\cdot]$ is the expectation operator.

Substituting equation (6) into equation (8) will obtain the following.

$$R_{iik}(T) = \sum_{r=1}^{n}\sum_{s=1}^{n} \varphi_{ir}\varphi_{kr}\varphi_{is}\varphi_{ks} \int_{-\infty}^{t}\int_{-\infty}^{t+T} g_r(t+T-\sigma) g_s(t-\tau) E\left[f_k(\sigma) f_k(\tau)\right]\mathrm{d}\sigma\mathrm{d}\tau, \tag{9}$$

where φ_{ir} is the r^{th} mode shape value at point i, φ_{kr} is the r^{th} mode shape value at point k, φ_{is} is the s^{th} mode shape value at point i, and φ_{ks} is the s^{th} mode shape value at point k. n is the number of DOFs. $g_r(t)$ is the impulse response function related to the r^{th} modal parameters. $g_s(t)$ is the impulse response function related to the s^{th} modal parameters.

Assuming that the excitation $f_k(t)$ at point k is Gaussian white noise, the autocorrelation function of excitation can be expressed as

$$R_{f_k f_k}(\tau-\sigma) = E\left[f_k(\sigma) f_k(\tau)\right] = \alpha_k\delta(\tau-\sigma), \tag{10}$$

where α_k is the coefficient depending on exciting point k, and $\delta(t)$ is the pulse function.

Substituting equation (10) into equation (9), and calculating the first integration by using the definition of $\delta(t)$, note that

$$R_{iik}(T) = \sum_{r=1}^{n}\sum_{s=1}^{n} \alpha_k\varphi_{ir}\varphi_{kr}\varphi_{is}\varphi_{ks} \int_{-\infty}^{t} g_r(t+T-\tau) g_s(t-\tau)d\tau. \tag{11}$$

Because $-\infty \leq \tau \leq t$, if we define $\lambda = t - \tau$, the limits of λ will be 0 to ∞. Then, the above equation (11) can be rewritten as

$$R_{iik}(T) = \sum_{r=1}^{n}\sum_{s=1}^{n} \alpha_k\varphi_{ir}\varphi_{kr}\varphi_{is}\varphi_{ks} \int_{0}^{\infty} g_r(\lambda+T) g_s(\lambda)\mathrm{d}\lambda. \tag{12}$$

Due to the definition of $g_r(t)$ from equation (7), equation (12) can be deformed into [30].

$$R_{iik}(T) = \sum_{r=1}^{n}\left[\left(A_{iik}^r e^{-\zeta_r(\omega_{nr}T)}\cos\left(\omega_{dr}T\right) + B_{iik}^r e^{-\zeta_r\omega_{nr}T}\sin\left(\omega_{dr}T\right)\right)\right], \tag{13}$$

where A_{iik}^r and B_{iik}^r are functions of the modal parameters.

$$A_{iik}^r = \sum_{s=1}^{n} \frac{\alpha_k\varphi_{ir}\varphi_{kr}\varphi_{is}\varphi_{ks}}{m_r\omega_{dr}m_s}\left[\frac{I_{rs}}{\left(J_{rs}^2 + I_{rs}^2\right)}\right], \tag{14}$$

$$B_{iik}^r = \sum_{s=1}^{n} \frac{\alpha_k\varphi_{ir}\varphi_{kr}\varphi_{is}\varphi_{ks}}{m_r\omega_{dr}m_s}\left[\frac{J_{rs}}{\left(J_{rs}^2 + I_{rs}^2\right)}\right], \tag{15}$$

where $I_{rs} = 2\omega_{dr}(\zeta_r\omega_{nr} + \zeta_s\omega_{ns})$ and $J_{rs} = (\omega_{ds}^2 - \omega_{dr}^2) + (\zeta_r\omega_{nr} + \zeta_s\omega_{ns})^2$.

As described in Ref. [30], define the variable γ_{rs} as follows:

$$\tan((\gamma_{rs})) = \frac{I_{rs}}{J_{rs}}. \tag{16}$$

Substitute equations (14) and (15) into equation (13), and simplify it to produce the autocorrelation function.

$$R_{iik}(T) = \sum_{r=1}^{n} \frac{\varphi_{ir}}{m_r\omega_{dr}} \sum_{s=1}^{n}\sum_{k=1}^{n} \frac{\alpha_k\varphi_{kr}\varphi_{is}\varphi_{ks}}{m_s}\left(J_{rs}^2 + I_{rs}^2\right)\left(\frac{-1}{2}\right)e^{-\zeta_r(\omega_{nr}T)}\sin(\omega_{dr}T + \gamma_{rs}), \tag{17}$$

Note that the inner summation on s and k is just the summation of constants multiplied by the sine function. In addition, its frequency ω_{dr} is fixed, and phase angel γ_{rs} is variable. Therefore, the inner summation on s and k can be rewritten as a new sine function with a new phase angel θ_r and a new constant multiplier G_{ir}.

$$\sum_{s=1}^{n}\sum_{k=1}^{n} \frac{\alpha_k\varphi_{kr}\varphi_{is}\varphi_{ks}}{m_s}\left(J_{rs}^2 + I_{rs}^2\right)^{-1/2}\sin(\omega_{dr}T + \gamma_{rs}) = G_{ir}\sin(\omega_{dr}T + \theta_r), \tag{18}$$

where $I_{rs} = 2\omega_{dr}(\zeta_r\omega_{nr} + \zeta_s\omega_{ns})$ and $J_{rs} = (\omega_{ds}^2 - \omega_{dr}^2) + (\zeta_r\omega_{nr} + \zeta_s\omega_{ns})^2$.

Based on equation (18), the above equation (17) can be further rewritten as

$$R_{iik}(T) = \sum_{r=1}^{n} \frac{\varphi_{ir}G_{ir}}{m_r\omega_{dr}}e^{-\zeta_r\omega_{nr}T}\sin(\omega_{dr}T + \theta_r), \tag{19}$$

where G_{ir} is the coefficient depending on r^{th} modal parameters and the response point i. θ_r is the phase angle depending on r^{th} modal parameters.

Consequently, it can be found from equation (19) that the autocorrelation function of the structural vibration displacement response is related to the structural modal parameters.

2.2. Definition of Looseness Damage Index. The structural looseness damage often changes the physical properties of the system. The looseness of bolted connections essentially causes the stiffness of the structure to decrease and ultimately leads to changes in the dynamic characteristics before and after the bolts are loose. Therefore, the bolt looseness can be detected based on the change of the dynamic characteristics caused by the looseness damage.

Considering that the autocorrelation function of each measuring point is related to the structural dynamic characteristic parameters in Section 2.1, when the time lag T is 0, equation (19) can be expressed as

$$R_{ii}(0) = \sum_{r=1}^{n} \frac{\varphi_{ir}G_{ir}}{m_r\omega_{dr}}\sin\theta_r, \tag{20}$$

where G_{ir} is the coefficient depending on r^{th} modal parameters and the response point i, and φ_{ir} is the r^{th} mode shape value at point i.

From equation (20), it is can be seen that the autocorrelation function value $R_{ii}(0)$ at time lag $T = 0$ is composed of parameters such as mode shape and modal frequency. Therefore, the autocorrelation function value at time lag $T = 0$ of the vibration response can be used for damage detection.

To reduce the influence of noise on the data results, it is usually necessary to obtain multiple sets of data under the same environment or segment the data obtained at one time. Then, the results of multiple sets of data are averaged for reducing the influence of noise. For this reason, this paper proposes using the average autocorrelation function $\overline{R_{ii}(0)}$ at time lag $T = 0$ to establish the looseness damage indicator, and its calculation equation is

$$\overline{R_{ii}(0)} = \frac{1}{K}\sum_{k=1}^{K} R_{x_kx_k}(0), \tag{21}$$

where K is the number of signal sets, $R_{x_kx_k}(0)$ is the autocorrelation function value at time lag $T = 0$ of the k^{th} collected data, and $\overline{R_{ii}(0)}$ is the average autocorrelation function value at time lag $T = 0$.

Therefore, the relative change degree of the average autocorrelation function value at time lag $T = 0$ is calculated, and the bolt looseness damage index can be established as

$$\delta = \frac{\left|\overline{R_{\text{damage}}(0)} - \overline{R_{\text{ok}}(0)}\right|}{\overline{R_{\text{ok}}(0)}}, \tag{22}$$

where δ is taken as the bolt looseness damage index, $\overline{R_{ok}(0)}$ is the average autocorrelation function value in tightened

state, and $\overline{R_{\text{damage}}(0)}$ is the average autocorrelation function value in loose state.

It can be seen from equation (22) that the larger the damage index δ, the greater the relative difference of the average autocorrelation function value before and after the bolts are loose, and the greater the possibility of bolt looseness. Apparently, the smaller the bolt looseness damage index δ, the smaller the relative difference of the average autocorrelation function value before and after the bolts are loose, and the less the possibility of bolt looseness. Therefore, the bolt corresponding to the maximum looseness damage index can be found out as the loose bolt.

2.3. Proposed Method and Procedures. Based on the above analysis, a new method for bolt looseness detection based on average autocorrelation function is proposed. The flow chart of the proposed method, as shown in Figure 1, can be summarized as follows.

(1) For the undamaged structure, obtain the vibration signal $x^{(m)}$ of the location near the bolt Bm under ambient excitation (we denoted these bolts as B1, B2, . . ., B $(L-1)$, and BL, $m = 1, 2, \ldots, L$), and continuously collect K sets of data under the same environment. Take the k^{th} set of data x_k as an example, x_k is $[x_{k1}, x_{k2}, \ldots, x_{(kN-1)}, x_{kN}]$, and use equation (23) to calculate the autocorrelation function value at time lag $T = 0$.

$$R_{x_k x_k}(0) = \frac{1}{N}\sum_{i=1}^{N} x_{ki}^2 = \frac{\left(x_{k1}^2 + x_{k2}^2 + \cdots + x_{(kN-1)}^2 + x_{kN}^2\right)}{N}. \tag{23}$$

(2) Average the autocorrelation function values of the K sets of data, and use equation (24) to calculate the average correlation function value at time lag $T = 0$.

$$\overline{R_{\text{ok}}^{(m)}(0)} = \frac{1}{K}\sum_{k=1}^{K} R_{x_k x_k}(0). \tag{24}$$

(3) For the damaged structure, obtain the vibration signal $y^{(m)}$ of the location near the bolt Bm under ambient excitation, and continuously collect K sets of data under the same environment. Take the k^{th} set of data y_k as an example, y_k is $[y_{k1}, y_{k2}, \ldots, y_{(kN-1)}, y_{kN}]$, and use equation (25) to calculate the autocorrelation function value at time lag $T = 0$.

$$R_{y_k y_k}(0) = \frac{1}{N}\sum_{i=1}^{N} y_{ki}^2 = \left(\frac{\left(y_{k1}^2 + y_{k2}^2 + \cdots + y_{(kN-1)}^2 + y_{kN}^2\right)}{N}\right). \tag{25}$$

(4) Average the autocorrelation function values of the K sets of data, and use equation (26) to calculate the average correlation function value at time lag $T = 0$.

$$\overline{R_{\text{damage}}^{(m)}(0)} = \frac{1}{K}\sum_{k=1}^{K} R_{y_k y_k}(0). \tag{26}$$

(5) Calculate the relative change degree δ of the average autocorrelation function value at time lag $T = 0$ before and after the bolts are loose.

$$\delta_m = \left(\frac{\left|\left(\overline{R_{\text{damage}}^{(m)}(0)} - \overline{R_{\text{ok}}^{((m))}(0)}\right)\right|}{\overline{R_{\text{ok}}^{(m)}(0)}}\right), \tag{27}$$

where $\overline{R_{\text{ok}}^{(m)}(0)}$ is the average autocorrelation function value at time lag $T = 0$ before the bolt is loose, $R_{\text{damage}}^{(m)}(0)$ is the average autocorrelation function value at time lag $T = 0$ after the bolt is loose, and m is the bolt number, $m = 1, 2, \ldots, L$.

(6) Repeat the above steps, and calculate the relative change degree δ of the average autocorrelation function value at time lag $T = 0$ of all bolts. And find out the bolt Bl corresponding to the maximum looseness index, and it is regarded as the loose bolt, $\delta_l = \max(\delta_1, \delta_2, \ldots, \delta_L)$.

3. Experimental Verification

3.1. Detecting System of Bolt Looseness Based on Computer Vision. In order to further verify the feasibility of the proposed method in this paper, the sketch of the detecting system of bolt looseness is shown in Figure 2. The detecting system mainly consists of three parts: bolted connection plate, the shaker with its control system, and vision-measurement system. Further, the shaker with its control system consists of a shaker, a power amplifier, and a computer equipped with the LMS Test.Lab software. The vision-measurement system consists of a camera, an optical lens, and a computer equipped with the image acquisition software.

In addition, Figure 3 shows the principle of vision-measurement system. a is the image distance. b is the object distance, and O is the optical center of the lens. A is the spatial position of the object when the object is stationary, and B is the projection position of the object on the imaging plane when the object is stationary.

As shown in Figure 3, we assume that the direction of movement of the object is parallel to the imaging plane. When the time $k\Delta t$ has passed, the object moves from A to A', and its displacement in space is denoted as x. Further, the projection position of the object will move from B to B', and its pixel displacement can be denoted as y. According to the similar triangle relationship in Figure 3 will find the following:

$$\frac{x}{y} = \frac{b}{a}. \tag{28}$$

If the time $k\Delta t$ is, respectively, $1\Delta t, 2\Delta t, \ldots, (N-1)\Delta t, N\Delta t$, the vibration signal of the object relative to the stationary position can be denoted as $x(t)$.

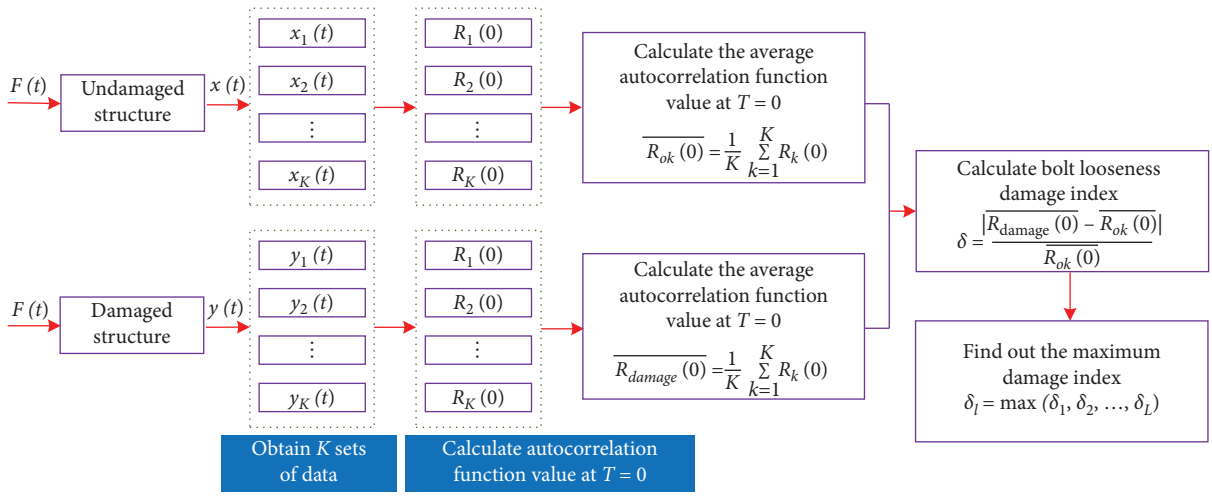

Figure 1: Flow chart of proposed method for bolt looseness detection.

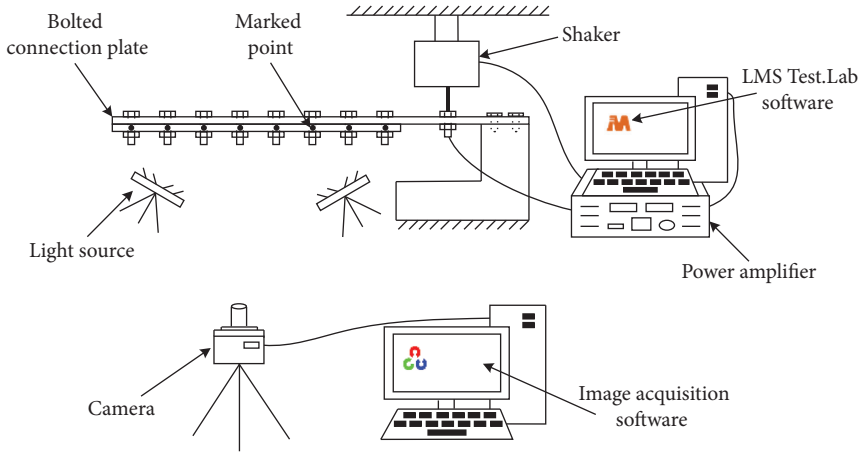

Figure 2: The sketch of the detecting system of bolt looseness.

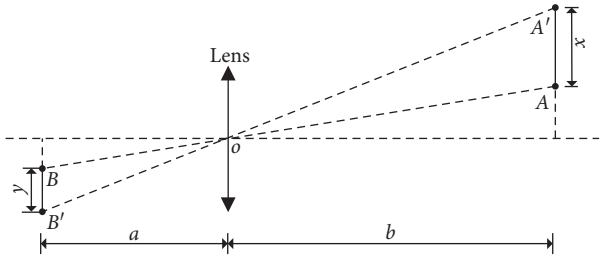

Figure 3: The principle of vision-measurement system.

Correspondingly, the pixel displacement signal of the object relative to the stationary position can be expressed as $y(t)$. Then, combining equation (28) will result in the following:

$$x(t) = \frac{b}{a} y(t). \tag{29}$$

If the relative position of the camera and the object is fixed, both a and b will be constant. According to equation (29), we can find that the actual vibration displacement $x(t)$ is linearly proportional to the pixel displacement $y(t)$, and their scale factor is b/a.

Based on the above analysis, when the bolt looseness damage index is calculated by equation (29), it can be seen that the scale factor b/a will be removed. Apparently, the damage index value calculated by using the pixel displacement is equal to the damage index value calculated by the actual displacement. Therefore, we can directly use the pixel displacement signal to calculate the bolt looseness damage index.

3.2. Experimental Setup. Figure 4 shows the experimental setup for bolt looseness detection, and the shaker and bolted connection plate are shown in detail in Figure 5. The bolted connection plate consists of an aluminum plate (size: 777 mm × 50 mm × 2 mm) and another aluminum plate (size: 510 mm × 50 mm × 2 mm) integrated by ten M6 bolts. In addition, the distance between the bolts is 50 mm, and we denoted these M6 bolts as B1, B2, . . ., B9, and B10. The experimental setup also consists of a shaker, a computer equipped with the LMS Test.Lab software, a power amplifier, and a vision-measurement system, as depicted in Figure 4. The vision-measurement system consists of a camera (IMI Tech/IMB-3213UP), an optical lens (TOKINA/TC1214-

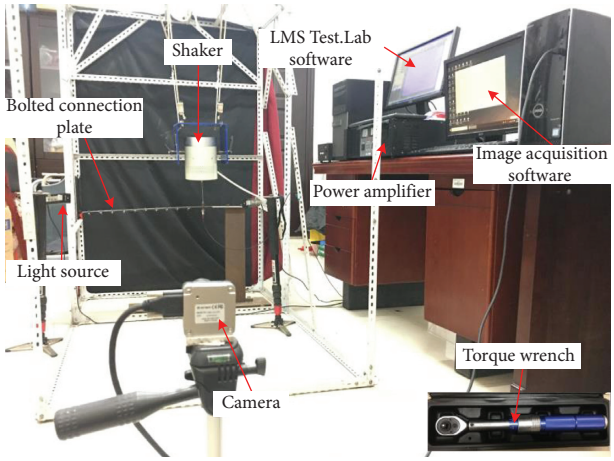

Figure 4: Experimental setup.

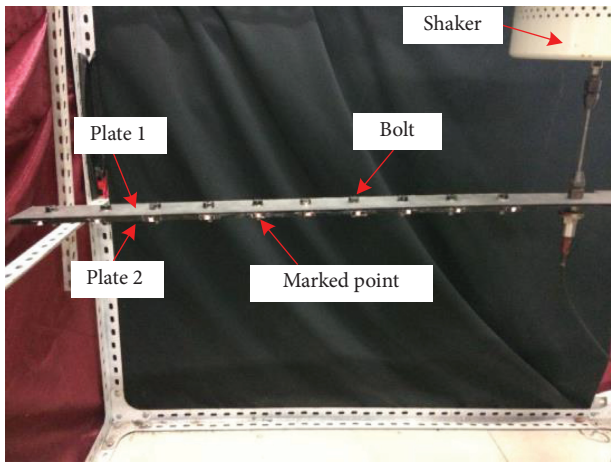

Figure 5: Shaker and bolted connection plate.

3MPG), and a computer equipped with the image acquisition software. The camera uses a CMOS sensor as the image receiver to collect 8-bit grayscale images at a speed of 300 fps. These images are transferred to the computer through the USB3.0 interface to obtain the vibration video signal. Table 1 shows the specific parameters of vision-measurement system.

The shaker is controlled by a computer, which is equipped with the LMS Test. Lab software. The driving signal can be manually set as an ambient excitation to drive the vibration of the bolted connection plate. The bottom right of Figure 4 is a torque wrench, which can be used to adjust the pretension force of the bolt. There are a total of ten M6 bolts on the bolted connection. Marked points are pasted near each bolt on the plate to establish eye-catching features, and we denoted these marked points as P1, P2, . . . , P9, and P10. As shown in Figure 6, we can see the position of the marked points from a partial image.

3.3. Experimental Method. To avoid the bolt pretension force from exceeding the aluminum material yield strength, when we use the torque wrench to set the pretension force to 3 N·m, the bolt is considered to be perfect integration. When the pretension force is set to 0 N·m, the bolt is considered to be complete looseness. When the pretension force is set to 1.5 N·m, the bolt is considered to be half looseness.

The Gaussian white noise excitation with the frequency from 15 to 36 Hz and duration 2 minutes is taken as an input in the experiment. In addition, the frame rate of camera is set to 300 fps. When the bolted connection plate is vibrating, a sequence of images can be recorded by the camera, and there is no need for camera calibration in this process. After obtaining the sequence of images, python and open source computer vision (OpenCV) libraries are used to process these images for obtaining the vibration pixel displacement signal of each marked point. Then, the relative difference of the average autocorrelation function value will be calculated. The following section gives detailed inspection results of different locations of bolt looseness.

4. Results and Discussion

4.1. Experiments for Bolt Looseness Location

4.1.1. Bolt B2 Looseness. The pixel displacement signal of each marked point in tightened state can be obtained, and 3 sets of data can be obtained continuously under the same environment. When the pretension force of bolt B2 is set to 0N·m (complete looseness) by a torque wrench, these pretension forces of other bolts are set to 3N·m.

The pixel displacement signal of each point in the loose state can be obtained by the vision-measurement system, and 3 sets of data can be obtained continuously. Taking the first set of data as an example, vibration pixel displacements at P1 are shown in Figure 7, where Figure 7(a) is the sample pixel displacement for the undamaged structure, and Figure 7(b) is pixel displacement for the structure of bolt B2 looseness.

By the above vibration pixel displacements at P1, the autocorrelation functions can be calculated. Figure 8 shows the autocorrelation function at P1 before and after damage.

Because the autocorrelation function of the structural vibration displacement response is related to the structural modal parameters, the autocorrelation function value at time lag $T = 0$ of each marked point is used to calculate the detection index. Finally, the histogram of bolt looseness damage index is shown in Figure 9.

From Figure 9, one observes that the looseness damage index of bolt B2 is the largest, which indicates that the relative change of the average autocorrelation function value at time lag $T = 0$ of bolt B2 is relatively large, while the relative changes of the average autocorrelation function value at time lag $T = 0$ of other bolts are relatively small. Consequently, it can be considered that bolt B2 has looseness. In fact, the actual looseness is achieved by adjusting the pretension force of bolt B2 to 0 N·m. Therefore, the detection result of the proposed method is consistent with the actual bolt looseness location.

4.1.2. Bolt B5 Looseness. To further verify the accuracy of the proposed method in this paper, correspondingly, the

Table 1: Specific parameters of vision-measurement system.

Component	Model	Specific parameters
Camera	IMI Tech/IMB-3213UP	Image sensor type: 1/3 CMOS Maximum resolution: 640×480 pixel Real frame rate: 300 fps Image: 8-bit grayscale Pixel size: $4.8 \times 4.8\,\mu$m Lens mount: C/CS-Mount Digital interface/Transfer rate: USB3.0/5 Gbps S/N ratio: 40 dB or better Dynamic range: 60 dB in global shutter mode
Optical lens	TOKINA/TC1214-3MPG	Focal length: 12 mm Aperture range: F1.4–16 Mount: C-mount Angle of view: $39.6^\circ \times 30.2^\circ$
Accessories	USB3.0 cable	

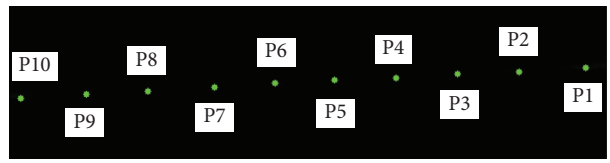

Figure 6: The position of the marked points.

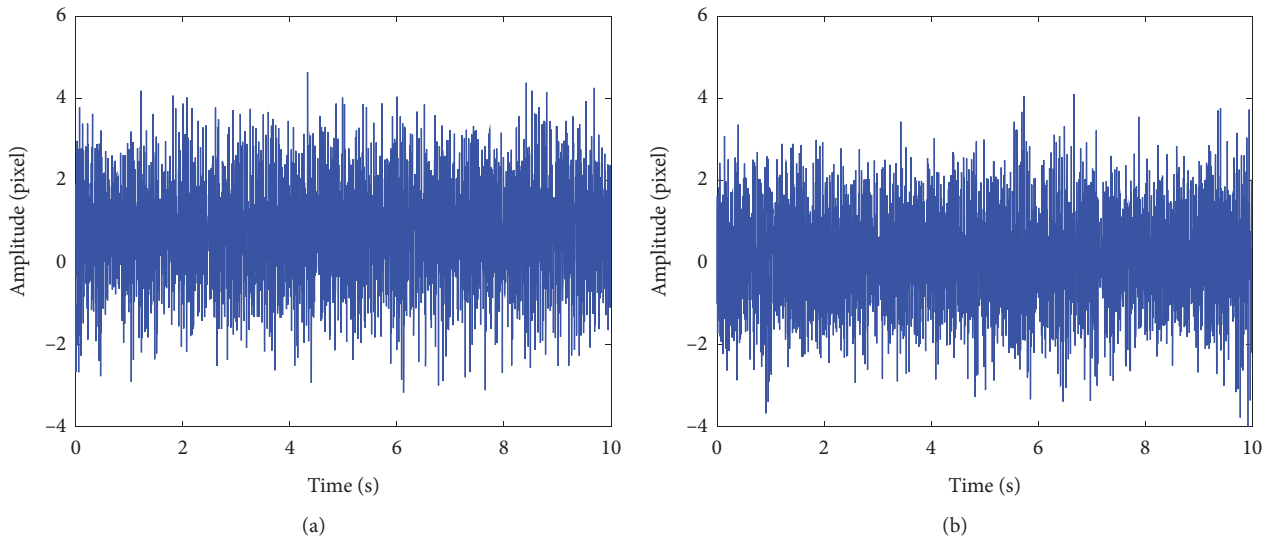

Figure 7: Vibration pixel displacements at P1. (a) Pixel displacement for the undamaged structure. (b) Pixel displacement for the structure of bolt B2 looseness.

pretension force of bolt B5 is set to 0 N·m (complete looseness) by a torque wrench, and pretension force of other bolts are set to 3 N·m. The pixel displacement signal of each point can be obtained by the vision-measurement system. Then, according to the flow chart of the proposed method described above, the histogram of the bolt looseness damage index can be shown in Figure 10.

As shown in Figure 10, the looseness damage index of bolt B5 is the largest, which indicates that the relative change of the average autocorrelation function value at time lag $T = 0$ of bolt B5 is relatively large. Consequently, it can be considered that bolt B5 has looseness. In fact, the actual looseness is achieved by adjusting the pretension force of bolt B5 to 0 N·m. Therefore, the detection result of the proposed method is consistent with the actual bolt looseness location.

4.1.3. Bolts B2 and B5 Looseness. When the pretension force of bolts B2 and B5 is set to 0 N·m (complete looseness) by the torque wrench, these pretension forces of other bolts are set to 3 N·m. The pixel displacement signal of each point can be

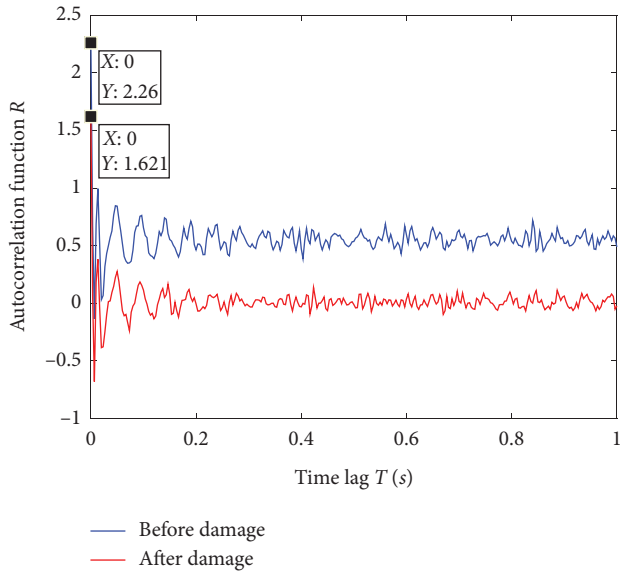

Figure 8: Autocorrelation function at P1.

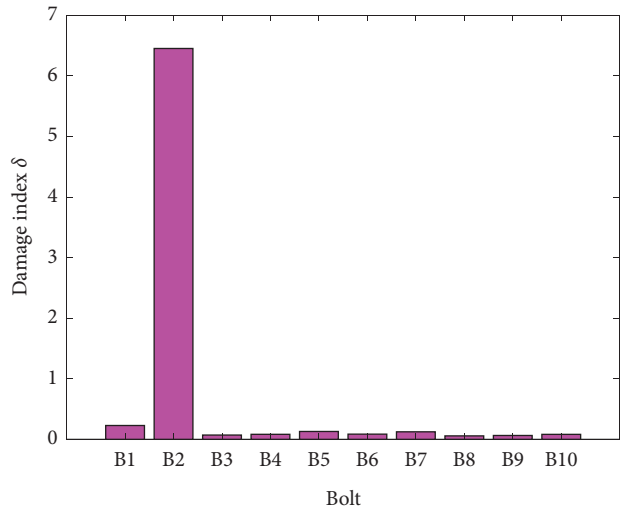

Figure 9: Histogram of bolt looseness damage index

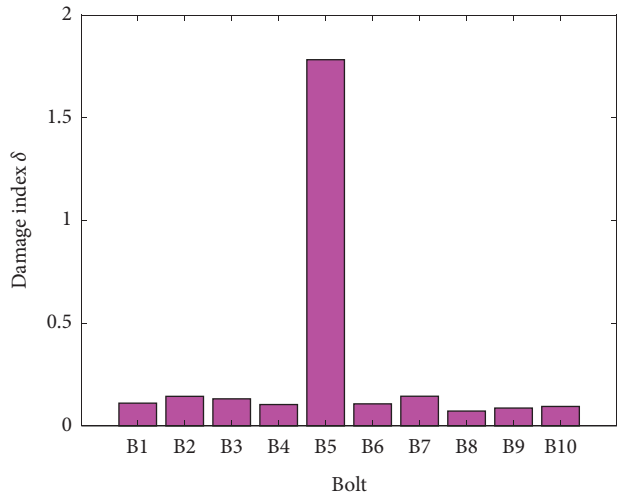

Figure 10: Histogram of bolt looseness damage index.

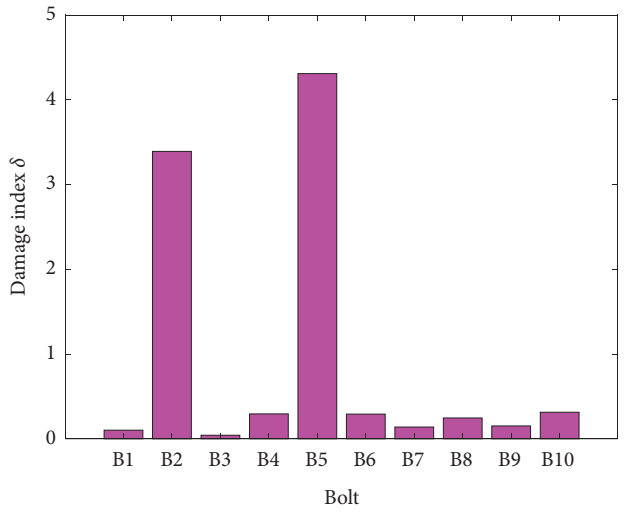

Figure 11: Histogram of bolt looseness damage index.

obtained by the vision-measurement system. According to the method flow described above, the histogram of the bolt looseness damage index can be shown in Figure 11.

From Figure 11, it can be seen that the looseness damage index of bolt B5 is the largest, followed by bolt B2, which indicates that the relative change of the average autocorrelation function value at time lag $T = 0$ of bolts B2 and B5 is relatively large. Consequently, it can be considered that bolts B2 and B5 have looseness. In fact, the actual looseness is achieved by adjusting the pretension force of bolts B2 and B5 to 0 N·m. Therefore, the detection result of the proposed method is consistent with the actual bolt looseness location.

4.2. Experiments for the Influence of Bolt Looseness Degree. To further explore the applicability of the proposed method, a verification experiment is carried out to study the influence of different looseness degrees. The pretension force of bolt B5 is set to 0N·m, 1.5N·m, and 1.8N·m to simulate, respectively, 100% looseness, 50% looseness, and 40% looseness. The procedure of experiment is carried out following the same procedure described in Section 3.2. Figure 12 shows the relationship of damage index for different looseness degrees.

As shown in Figure 12, the damage index value changes with the change of the looseness degree. It also can be seen that the damage index value of bolt B5 in the state of complete looseness is larger than the damage index value in the state of 50% looseness. It shows that the smaller the pretension force, the greater the looseness degree. And the greater the relative difference of its autocorrelation function at time lag $T = 0$, the greater the damage index. In addition, from Figure 12, it also can be seen that the damage index is basically proportional to the level of the looseness.

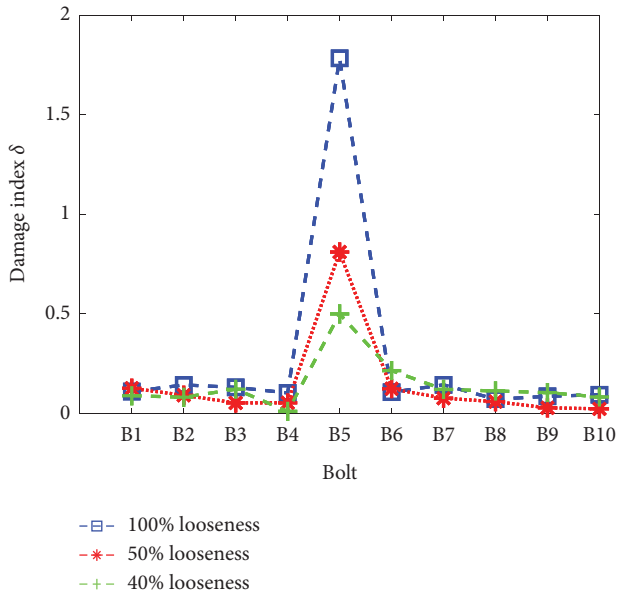

Figure 12: The relationship of damage index for different looseness degrees.

5. Conclusions

In this research, a new method for bolt looseness detection based on average autocorrelation function was proposed. It did not usually directly use the original response signal to extract the looseness damage features but used the average autocorrelation function value at time lag $T = 0$ of the original signal to establish the looseness damage index. By comparing the relative changes of each bolt looseness damage index, the bolt corresponding to the maximum looseness damage index could be denoted as the loose bolt. An experimental system for bolt looseness detection based on computer vision was designed. Validation experiments were carried out to demonstrate the feasibility of the proposed method, in which different bolt looseness locations and degrees were evaluated. Last but not least, this proposed method could be extended to other complex equipment structures with bolted connections.

Data Availability

The data and the MATLAB programs used to support the findings of this study are available from the corresponding author upon request.

Conflicts of Interest

The authors declare that there are no conflicts of interest regarding the publication of this paper.

Acknowledgments

This project was supported by the National Natural Science Foundation of China (Grant no. 51775181).

References

[1] S. M. Y. Nikravesh and M. Goudarzi, "A review paper on looseness detection methods in bolted structures," *Latin American Journal of Solids and Structures*, vol. 14, no. 12, pp. 2153–2176, 2017.

[2] F. Wang, S. C. M. Ho, and G. Song, "Modeling and analysis of an impact-acoustic method for bolt looseness identification," *Mechanical Systems and Signal Processing*, vol. 133, pp. 1–12, 2019.

[3] F. Wang and G. Song, "Bolt-looseness detection by a new percussion-based method using multifractal analysis and gradient boosting decision tree," *Structural Health Monitoring*, vol. 19, no. 6, pp. 2023–2032, 2020.

[4] Q. Li and X. Jing, "Fault diagnosis of bolt loosening in structures with a novel second-order output spectrum-based method," *Structural Health Monitoring*, vol. 19, no. 1, pp. 123–141, 2020.

[5] T. Panidis, I. Pavelko, V. Pavelko, S. Kuznetsov, and I. Ozolinsh, "Bolt-joint structural health monitoring by the method of electromechanical impedance," *Aircraft Engineering and Aerospace Technology*, vol. 86, no. 3, pp. 207–214, 2014.

[6] J. Min, S. Park, C.-B. Yun, C.-G. Lee, and C. Lee, "Impedance-based structural health monitoring incorporating neural network technique for identification of damage type and severity," *Engineering Structures*, vol. 39, pp. 210–220, 2012.

[7] J. Xu, J. Dong, H. Li, C. Zhang, and S. C. Ho, "Looseness monitoring of bolted spherical joint connection using electromechanical impedance technique and BP neural networks," *Sensors*, vol. 19, no. 8, pp. 1–19, 2019.

[8] P. Razi, R. A. Esmaeel, and F. Taheri, "Application of a remote health monitoring system for pipeline bolted Joints," *Proceedings of the ASME 2012 Pressure Vessels and Piping Conference*, vol. 9, pp. 121–129, 2012.

[9] J. J. Meyer and D. E. Adams, "Using impact modulation to quantify nonlinearities associated with bolt loosening with applications to satellite structures," *Mechanical Systems and Signal Processing*, vol. 116, pp. 787–795, 2019.

[10] Z. Zhang, M. Liu, Z. Su, and Y. Xiao, "Quantitative evaluation of residual torque of a loose bolt based on wave energy dissipation and vibro-acoustic modulation: a comparative study," *Journal of Sound and Vibration*, vol. 383, pp. 156–170, 2016.

[11] N. Zhao, L. Huo, and G. Song, "A nonlinear ultrasonic method for real-time bolt looseness monitoring using PZT transducer-enabled vibro-acoustic modulation," *Journal of Intelligent Material Systems and Structures*, vol. 31, no. 3, pp. 364–376, 2020.

[12] F. Wang and G. Song, "Bolt early looseness monitoring using modified vibro-acoustic modulation by time-reversal," *Mechanical Systems and Signal Processing*, vol. 130, pp. 349–360, 2019.

[13] Z. Zhang, M. Liu, Y. Liao, Z. Su, and Y. Xiao, "Contact acoustic nonlinearity (CAN)-based continuous monitoring of bolt loosening: hybrid use of high-order harmonics and spectral sidebands," *Mechanical Systems and Signal Processing*, vol. 103, pp. 280–294, 2018.

[14] Y.-K. An and H. Sohn, "Integrated impedance and guided wave based damage detection," *Mechanical Systems and Signal Processing*, vol. 28, pp. 50–62, 2012.

[15] J.-W. Lee, "Bolt-joint structural health monitoring technique using transfer impedance," *Journal of the Korea Academia-*

Industrial Cooperation Society, vol. 20, no. 7, pp. 387–392, 2019.

[16] W. Sun and Y. Zhang, "Numerical simulation of bolt looseness monitoring based on impedance method," *Applied Mechanics and Materials*, vol. 351-352, pp. 1264–1268, 2013.

[17] P. Razi, R. A. Esmaeel, and F. Taheri, "Improvement of a vibration-based damage detection approach for health monitoring of bolted flange joints in pipelines," *Structural Health Monitoringl*, vol. 12, no. 3, pp. 207–224, 2013.

[18] F. Huda, I. Kajiwara, N. Hosoya, and S. Kawamura, "Bolt loosening analysis and diagnosis by non-contact laser excitation vibration tests," *Mechanical Systems and Signal Processing*, vol. 40, no. 2, pp. 589–604, 2013.

[19] R. A. Esmaeel, J. Briand, and F. Taheri, "Computational simulation and experimental verification of a new vibration-based structural health monitoring approach using piezoelectric sensors," *Structural Health Monitoring*, vol. 11, no. 2, pp. 237–250, 2012.

[20] M. Zhang, Y. Shen, L. Xiao, and W. Qu, "Application of subharmonic resonance for the detection of bolted joint looseness," *Nonlinear Dynamics*, vol. 88, no. 3, pp. 1643–1653, 2017.

[21] F. Amerini and M. Meo, "Structural health monitoring of bolted joints using linear and nonlinear acoustic/ultrasound methods," *Structural Health Monitoring*, vol. 10, no. 6, pp. 659–672, 2011.

[22] G. P. M. Fierro and M. Meo, "IWSHM 2017: structural health monitoring of the loosening in a multi-bolt structure using linear and modulated nonlinear ultrasound acoustic moments approach," *Structural Health Monitoring*, vol. 17, no. 6, pp. 1349–1364, 2018.

[23] S. M. Y. Nikravesh and M. Goudarzi, "Experimental and numerical looseness detection and assessment in flanged joints using vibro-acoustic modulation method," *Mechanics Based Design of Structures and Machines*, vol. 48, no. 6, pp. 1–17, 2020.

[24] X. He and T. She, "A New Identification Method for Bolt Looseness in Wind Turbine Towers," *Shock and Vibration*, vol. 2019, Article ID 6056181, 10 pages, 2019.

[25] W. Zhou, Y. Shen, L. Xiao, and W. Qu, "Application of nonlinear-modulation technique for the detection of bolt loosening in frame structure," *Journal of Testing and Evaluation*, vol. 44, no. 2, pp. 967–975, 2016.

[26] R. Chen, S. Chen, L. Yang, J. Wang, X. Xu, and T. Luo, "Looseness diagnosis method for connecting bolt of fan foundation based on sensitive mixed-domain features of excitation-response and manifold learning," *Neurocomputing*, vol. 219, pp. 376–388, 2017.

[27] N. G. Pnevmatikos, B. Blachowski, G. Hatzigeorgiou, and A. Swiercz, "Wavelet analysis based damage localization in steel frames with bolted connections," *Smart Structures and Systems*, vol. 18, no. 6, pp. 1189–1202, 2016.

[28] K. He and W. D. Zhu, "Detecting loosening of bolted connections in a pipeline using changes in natural frequencies," *Journal of Vibration and Acoustics*, vol. 136, no. 3, pp. 1–8, 2014.

[29] A. Milanese, P. Marzocca, J. M. Nichols, M. Seaver, and S. T. Trickey, "Modeling and detection of joint loosening using output-only broad-band vibration data," *Structural Health Monitoring*, vol. 7, no. 4, pp. 309–328, 2008.

[30] G. H. James, T. G. Carne, and J. P. Lauffer, "The natural excitation technique (NExT) for modal parameter extraction from operating structures," *Modal Analysis: The International Journal of Analytical and Experimental Modal Analysis*, vol. 10, no. 4, pp. 260–277, 1995.

[31] C. R. Farrar and G. H. James III, "System identification from ambient vibration measurements on a bridge," *Journal of Sound and Vibration*, vol. 205, no. 1, pp. 1–18, 1997.